12-1-2012

Comparison and Simulation of Salt-Ceramic Composites for Use in High Temperature Concentrated Solar Power

Lauren Michelle Fossile
University of Nevada, Las Vegas

Follow this and additional works at: https://digitalscholarship.unlv.edu/thesesdissertations

Part of the Ceramic Materials Commons, and the Oil, Gas, and Energy Commons

COMPARISON AND SIMULATION OF SALT-CERAMIC COMPOSITES FOR USE IN

HIGH TEMPERATURE CONCENTRATED SOLAR POWER

By

Lauren Michelle Fossile

Bachelor of Science in Materials Engineering

California Polytechnic State University

2008

A thesis submitted in partial fulfillment of the requirements for the

Master of Science in Mechanical Engineering

Mechanical Engineering Department

College of Engineering

The Graduate College

University of Nevada, Las Vegas

December 2012

UNLV
UNIVERSITY OF NEVADA LAS VEGAS

THE GRADUATE COLLEGE

We recommend the thesis prepared under our supervision by

Lauren Fossile

entitled

Comparison and Simulation of Salt-Ceramic Composites for Use in High Temperature Concentrated Solar Power

be accepted in partial fulfillment of the requirements for the degree of

Master of Science in Mechanical Engineering
Department of Mechanical Engineering

Robert Boehm, Committee Chair

Yi-Tung Chen, Committee Member

Brendan O'Toole, Committee Member

William J. Smith, Jr., Graduate College Representative

Thomas Piechota, Ph. D., Interim Vice President for Research and Graduate Studies and Dean of the Graduate College

December 2012

Abstract

Due to the inherently intermittent nature of solar energy caused by cloud cover among other sources, thermal storage systems are needed to make solar energy more consistent. This same technology could be used to prolong the daily number of useful hours of solar energy power plants. Salt-ceramic materials are a relatively new prospect for heat storage, but have been researched mostly with magnesium oxide and several different carbonate salts. Salt ceramics are a phase change material where the salt changes phase inside the ceramic structure allowing for the system to use the sensible heat of both materials and the latent heat of the salt to store thermal energy. Capillary forces within the ceramic structure hold in the salt when the salt melts.

The focus here is on the possibility of creating a low-cost salt-ceramic storage material for high temperature solar energy applications. A theoretical analysis of the resulting materials is performed. While most of the existing salt ceramics have been made from magnesium oxide, aluminum oxide is more readily available from various companies in the area. Magnesium oxide is often considered a custom ceramic, so it is more expensive. A cost and material property comparison has been completed between these two materials to determine which is better suited for solar storage. Many of the existing salt-ceramics use carbonate salts, but nitrate salts are commonly used in graphite/salt composites. Therefore, a cost and theoretical performance comparison is between these materials also. For comparisons' sake, zirconia and graphite have also been analyzed as the filler in the composite. Each combination of salt and ceramic or graphite has been analyzed.

In order to make the use of salt-ceramics more cost-effective and available to Nevada's energy providers, research has been done into which ceramics have high availability in Nevada, low cost, and the best material properties for this application. The thermal properties and cost of these materials have been compared to the price that Nevada's energy utilities are willing to pay per unit of stored energy, which was approximated through a survey conducted by the National Science Foundation (NSF)– Experimental Project to Stimulate Competitive Research (EPSCoR) at the University of Nevada, Las Vegas. The surveys were completed on Nevadan energy purveyors concerning climate change attitudes, but included questions regarding the usefulness and cost of solar storage.

The cost per unit of energy has also been calculated and whether the utilities would be willing to pay for each combination will be determined using information obtained from the surveys mentioned above. This information will dictate which combination will be best for use in the state of Nevada at solar energy power plants.

Acknowledgements

I would like to acknowledge my advisory committee chair, Dr. Bob Boehm, for his help and unwavering optimism. He kept me on task and asked the necessary questions so that I could learn from my mistakes.

I would also like to acknowledge the help of the rest of my advisory committee, Dr. Yitung Chen, Dr. Brendan O'Toole, and Dr. William J. Smith, Jr. Dr. Chen has been a fantastic teacher who challenged me to think and be creative in attacking a problem. Dr. O'Toole always made equipment available to me when I needed a furnace or a thermocouple. Dr. Smith made sure I had his support through every step of this process. They have all been invaluable.

Dr. Thomas Piechota and Dr. William J. Smith, Jr. worked with me in the Experimental Program to Stimulate Competitive Research (EPSCoR) grant through the National Science Foundation. Through EPSCoR, the surveys used in the cost analysis of thesis were conducted. So the grant and the professors in charge must be acknowledged along with the post-doctorate faculty, and the graduate students.

Table of Contents

List of Figures

Chapter One

Literature Review

Phase change materials, including salt-ceramics and graphite-based composites, and effective thermal properties of composites have been highly researched. Their use for various purposes, including solar energy applications, is documented in the literature. A brief summary of some of this work follows.

Overview of Solar Energy and Storage Media

There are four basic types of concentrating solar power: parabolic trough, linear Fresnel, solar tower, and dish Stirling. The solar tower will see temperatures in the range of 300°C-2000°C. The power tower is also known to be extremely good for thermal storage (Barlev, 2011).

Storage materials have commonly been sensible heat materials that simply have high heat capacity. Many molten salts in the right temperature range can be used for sensible heat storage. Solids, like concrete or rocks, are commonly used to store sensible heat. Certain oils are used for sensible heat storage also. Phase change materials use the latent heat within the material to store more heat than the material could hold as sensible heat. When a salt melts, more energy is used and then stored as long as the salt is molten. When the salt cools, that heat is then released. In this situation, both sensible heat and latent heat can be used (Demirbas, 2006).

When temperatures are not conducive to water being used as a heat transfer fluid, other molten salts are often used instead. A mixture of fluoride salts, like

lithium fluoride, sodium fluoride, and potassium fluoride (FLiNaK), is a relatively

common salt for use at high temperatures (Forsberg et al., 2007).

Salt Studies

Salts have been studied to ascertain properties and for use in various

applications. A compilation of results from several studies was put together for the

density, heat capacity, thermal diffusivity, and thermal conductivity of sodium

nitrate. The density and heat capacity from several sources matched up well, but the

thermal conductivity and thermal diffusivity from multiple sources were scattered.

This study mainly added data to the thermal properties of sodium nitrate (Bauer et

al., 2012).

The thermal conductivity for potassium nitrate, lithium nitrate, lithium

carbonate, sodium nitrate, and sodium carbonate were available over a small range

of temperatures, along with the thermal conductivity of many other liquid inorganic

compounds (Yaws, 2009). Another study investigated potassium nitrate for thermal

properties. The heat capacity, thermal conductivity, and thermal diffusivity were all

measured for the range of temperatures of 300-500K (Taha et al., 1991). Yet

another study investigated the heat capacity, enthalpy, and entropy of lithium

carbonate for the temperatures of 303.15-563.15K (Kourkova et al., 2007). A molten

salt combination was investigated for thermal use and involved equations for the

heat capacity of sodium carbonate (Lindberg et al., 2007). High temperature phase

change materials were studied which involved compiling melting temperatures and

latent heat values for many salts including sodium carbonate, sodium nitrate, potassium nitrate, lithium carbonate, and lithium nitrate (Kenisarin, 2010).

A common tool in using molten salts is creating a eutectic by combining salts. An experiment with thirty-six different combinations of lithium carbonate, potassium carbonate, and sodium carbonate was completed. Several of the combinations did not form a eutectic. The melting temperature, cost, and latent heat were analyzed. The combinations with the highest percentages of lithium carbonate also had the highest prices per kilowatt-hour. The study involved calculating these properties, but not looking into which combination is truly best for the application. More research is needed before these salt combinations are ready for practical use (Ren et al., 2011). A very similar study focused on combinations of salts of the same constituents (sodium carbonate, lithium carbonate, and potassium carbonate), but for sensible heat use. The same pricing equation was used and the carbonate mixtures were compared by price and storage capacity. The conclusion was that further research must be completed (Wu et al., 2011).

Ceramic and Graphite Studies

The heat capacity of zirconia from 13K to 300K was measured in one study. At low temperatures, some variations between this study's results and previous studies exist (Tojo et al., 1999). Heat capacity equations for graphite and other graphite compounds were displayed in another study (Skoropanov et al., 1984). The thermal conductivity of magnesium oxide was measured and published in Slifka et al. (1998). The thermal conductivity and heat capacity of magnesia, alumina, and

zirconia were all available as data in a study looking into magnesia concerning thermal uses (Zabolotskii, 2011).

Another study concerned the use of graphite for chemical heat pumps. The density and thermal conductivity of the graphite was extremely important (Han et al., 1998). The thermal conductivity of graphite and alumina, as well as many other solid inorganic compounds, is available in Yaws (2009).

Salt-Ceramic Studies

Composites comprised of magnesia and either sodium carbonate, potassium carbonate, or lithium carbonate were compared for the purpose of thermal storage in a solar reformer. The percentage by weight was varied, but in each situation, the salt comprised a larger percentage by weight. For this study, a sintering process was used to create each sample after the components have been mixed together until homogenous as powders. The study found that the percentage of magnesia affected the overall thermal conductivity of the composite, and that the composite made of sodium carbonate and magnesia was the "most promising" at either eighty or ninety percent sodium carbonate (Gokon et al., 2009).

A new method of creating a salt-ceramic called "spontaneous melt-infiltration" was investigated. For this study, a salt-ceramic material was created using sodium sulfate and silicon dioxide. This salt ceramic is not a common combination among the researched composites. The temperature analysis considered for this situation focused on the structure and each component of the

composite instead of calculating effective properties that could then be input into a more generic equation (Huang et al., 2009).

Graphite/Molten Salt Studies

The main problem with molten salt phase change materials is a low thermal conductivity. The solution to this problem was hypothesized as dispersing graphite powder or flakes throughout the salt and possibly adding graphite fins to the structure. The graphite for this study was combined with sodium nitrate, potassium nitrate, sodium hydroxide, potassium hydroxide, zinc chloride, sodium nitrate combined with potassium nitrate, or zinc chloride combined with potassium chloride. The thermal conductivity of each sample was measured, while an equation was used to find the overall effective heat capacity. These properties were then used to simulate the temperature of the composite over time. The presence of the graphite was found to lower the latent heat of the salt by a small amount. The graphite was found to increase the thermal conductivity of the composite over use of only the salt (Pincemin et al., 2007).

Cold compression was used to form a composite with graphite and a molten salt comprised of both potassium nitrate and sodium nitrate. With the graphite included, the thermal conductivity was approximately twenty times greater overall. In this study, unlike the Pincemin et al. (2007) study, the latent heat was not affected. Also, the melting temperature of the salt was not affected by the addition of the graphite. On top of improving the necessary thermal properties, the overall cost of investment should decline when using graphite. According to the analysis

completed, in order to store the same amount of energy, a shorter length of tubes for the heat transfer fluid is needed. Therefore, the overall investment cause would decrease as opposed to a system without the graphite (Lopez et al., 2010).

Sodium nitrate, potassium nitrate, and a combination of the two salts were used to make composites with graphite. The composite samples were created using compression and infiltration methods. Once the samples were made, a laser-flash method was used to find the thermal conductivity of each composite. The comparison between this method and the real composite properties and behavior showed that the laser-flash method estimated the thermal conductivity extremely well. Thermal cycling of each sample showed that mass loss was not a concern (Bauer et al., unpublished).

Composite Formation Methods

The composites made for use as a thermal storage material are created using various methods. Gokon et al. (2009) as discussed above, used sintering to create the magnesia composites, which appears to be the most common method. Huang et al. (2009) used the "spontaneous melt-infiltration method," which involved using a ceramic preform. This method was new for this application and was not found to be common in making a thermal storage composite. Pincemin et al. (2008) simply dispersed the graphite flakes or powder into the salt. Lopez et al. (2010) used and compared cold compression methods, where compressing the material at room temperature formed the composite. This study was on graphite-based composites, but salt-ceramics would need more than just cold compression. Bauer et al. used

compression and infiltration methods. The compression was done at room temperature much like the Lopez et al. study. The infiltration was accomplished where the molten salt was poured into a porous graphite structure.

Corrosion

Molten salts are commonly corrosive so methods of reducing corrosion are important. Most nitrate salts are likely to cause intrinsic corrosion, but this is unlikely with other molten salts. Other salts have oxidation issues, like hydrogen fluoride and hydrogen chloride, where the salt reacts with reducible ions of the surrounding material. Sometimes, the thermal gradient inherent within the storage system can create solubility variations that allow for the formation of a "metal ion concentration cell." Lastly, most molten salts are electrically conductive and can connect materials allowing oxidation. Most of these corrosion mechanisms can be avoided simply by using coatings of nickel, carbon or molybdenum (Sabharwall et al., 2010).

Effective Thermal Property Calculations

The Maxwell-Eucken model for estimating the effective thermal conductivity of composites has been used in order to build a model that incorporates all general structural types of calculating effective thermal conductivity in composites. The general equation used in the Maxwell-Eucken model is:

$$K_{effective} = \frac{k_1 v_1 + k_2 v_2 \left(\frac{2k_1}{2k_1 + k_2}\right)}{v_1 + v_2 \left(\frac{3k_1}{2k_1 + k_2}\right)} \qquad (1)$$

In this equation, k_1 is the thermal conductivity of the continuous phase, k_2 is the thermal conductivity of the dispersed phase, v_1 is the volume fraction of the continuous phase, and v_2 is the volume fraction of the dispersed phase. This model assumes that small spheres are throughout the continuous phase and that the spheres are far enough apart not to thermally affect each other. The end equations are quite tedious however (Wang et al., 2006).

Many different models for calculating effective thermal conductivity of composites of various structures and phases have been reviewed. By comparing the output of the model and real world calculations, the Lewis-Nielson model was found to be the best model for a composite made of two solids (Progelhof et al., 1976).

The study by Pal (2008) used the Lewis-Nielson model to calculate the effective thermal conductivity of a composite using the structure of the composite, the thermal conductivity of each component and the volume fraction of each component. The model was found to work well when the composite is particulate-filled. The model's equations are described in more detail in Chapter 2.

Pincemin et al. (2008) used a complicated system to calculate the effective heat capacity. This method took into consideration the latent heat and the temperature range over which the phase transition occurred.

In order to calculate the effective heat capacity, Bauer et al. (unpublished) used simple equations for the effective density and effective heat capacity of composites.

Thermal Analysis of a Composite System

Simplified models were created in order to analyze different types of thermal energy storage. One type of storage system that was analyzed is a phase change material with tubes for the heat transfer fluid imbedded in the material. This system took into account both the convection from the moving heat transfer fluid and the conduction through the phase change material. However, in most situations, the conduction term is small enough to be disregarded. The system assumed a cylindrical tank containing the phase change material, which could be solid, liquid, or a mixture of the two. Within the phase change material were tubes imbedded of diameter .05 meters through which a heat transfer fluid would flow. The temperature equation found was:

$$hS_S(T_S - T_f)dz - (1 - \varepsilon)\pi R^2 k_s \left(\frac{\partial^2 T_S}{\partial z^2}\right)dz = -\rho_S C_S(1 - \varepsilon)\pi R^2 dz \left(\frac{\partial T_S}{\partial t}\right) \quad (2)$$

For this equation, T_S is the storage medium temperature, T_f is the fluid temperature, h is the heat transfer coefficient, S_S is the area of heat transfer surface per unit length, z is the position along the length of the tank, ε is the area of the tank taken up by the tubes for the heat transfer fluid, R is the radius of the tank, k_S is the thermal conductivity of the storage medium, ρ_S is the density of the storage medium, and C_S is the heat capacity of the storage medium. An equation to estimate the effectiveness of the system is also investigated (Li et al., 2012).

Kaminski considered governing heat equations and allowed the composite to be viewed as a homogenous block. In order to allow for the analysis, the thermal properties were assumed to be independent of temperature, and no phase change was assumed to occur over the temperature range being considered. The

'homogenized' behavior was found to be similar to the thermal behavior of the actual composite (Kaminski, 2002).

Since the conduction is generally assumed inconsequential, the model can be simplified further. In Duffie and Beckman (2006), an energy storage model is built off of the following two equations:

$$\frac{\delta T_f}{\delta x} = \left(\frac{UP}{(\dot{m}C_p)_f}\right)(T - T_f) \tag{3}$$

$$\frac{\delta u}{\delta t} = \left(\frac{UP}{\rho A}\right)(T_f - T) \tag{4}$$

In this set of equations, T_f is the heat transfer fluid temperature, T is the storage medium temperature, U is the overall heat loss coefficient, P is the perimeter, $\dot{m}$ is the mass flow rate of the heat transfer fluid, C_p is the heat capacity of the heat transfer fluid, u is the internal energy of the storage medium, ρ is the density of the storage medium, and A is the area of heat transfer. The equations are detailed more in Chapter Two.

Cost Analysis

The price of storage materials is simplified in the studies comparing the carbonate salt mixtures. The price per kilowatt-hour is meant to determine how much the material itself costs per kilowatt-hour that it can store based on the thermal properties. If Q is the amount of energy that the material can store over a set temperature range in kilowatt-hours per kilogram and P is the price of the material per unit mass given the percentage comprised of each component in dollars per kilogram, then the price per kilowatt-hour of the material is given by:

$$Price = \frac{P}{Q} \tag{5}$$

The price is then the most simplistic version since it does not incorporate the price of the system or the price of power that is bought (Ren et al., 2011; Wu et al., 2011). This is also only a present time price and does not take into account depreciation.

Chapter Two

Analysis

For this study, the salt-ceramics are assumed to be sintered composites made with 20 percent by weight of ceramic. The salt-ceramic once created would appear as a ceramic block (Gokon et al., 2009). The ceramics compared in this study are alumina, magnesia, and zirconia. Graphite is also compared to the ceramics, because of the amount of research into using graphite in the same manner as the ceramics (Lopez et al., 2010; Pincemin et al., 2008). The salts compared in this study are sodium nitrate, potassium nitrate, lithium nitrate, sodium carbonate, and lithium carbonate. Each possible combination of the possible salt and ceramic or graphite composite is analyzed.

The phases of the composite structure have known properties, but in order to assess its use as the storage medium, effective properties of each composite must be calculated. Both the effective thermal conductivity and the specific heat are needed for the solar analysis so that the different material combinations may be compared. Geometry must be assumed for the storage system before any thermal analysis can be done.

Thermal Conductivity

The Lewis-Nielsen equation is used for calculating the effective thermal conductivity. In this estimation, the thermal conductivity of each of the phases, the volume fraction of particles in the composite, and the general organization of the composite's structure are needed.

$$K_{Composite} = K_{Salt} \left(\frac{1+AB\phi_{Ceramic}}{1-B\psi\phi_{Ceramic}} \right) \tag{6}$$

where:

$$B = \left(\frac{\lambda-1}{\lambda+A} \right) \tag{6a}$$

$$\lambda = K_{Ceramic}/K_{Salt} \tag{6b}$$

$$A = k_E - 1 \tag{6c}$$

$$\psi = 1 + \left(\frac{1-\phi_m}{\phi_m^2} \right) \phi_{Ceramic} \tag{6d}$$

For this set of equations, $K_{Composite}$ is the effective thermal conductivity of the composite, K_{Salt} is the thermal conductivity of the salt, $K_{Ceramic}$ is the thermal conductivity of the ceramic or graphite, and $\phi_{Ceramic}$ is the volume fraction of the ceramic. For the organization of the composite, ϕ_m (maximum packing volume fraction) is 0.637 assuming that the composite is made of randomly closely packed spheres and k_E (Einstein coefficient) is 2.5 for spheres (Progelhof, 1976; Pal, 2008).

Specific Heat Capacity

The effective heat capacity is found using a calculation concerning the specific heat capacity, the density, and the volume fraction of each component.

$$C_{p,Composite} = \frac{\rho_{Salt}\, C_{p,Salt}\, \phi_{Salt} + \rho_{Ceramic}\, C_{p,Ceramic}\, \phi_{Ceramic}}{\rho_{Composite}} \tag{7}$$

where:

$$\rho_{Composite} = \rho_{Salt}\, \phi_{Salt} + \rho_{Ceramic}\, \phi_{Ceramic} \tag{7a}$$

In this set of equations, $C_{P,Composite}$ is the effective specific heat capacity of the composite, $C_{P,Salt}$ is the specific heat capacity of the salt, $C_{P,Ceramic}$ is the specific heat capacity of the ceramic or the graphite, $\rho_{Coposite}$ is the effective density of the

composite, ρ_{Salt} is the density of the salt, $\rho_{Ceramic}$ is the density of the ceramic, ϕ_{Salt} is the volume fraction of salt in the composite, and $\phi_{Ceramic}$ is the volume fraction of the ceramic in the composite (Bauer et al., unpublished).

Geometry of Storage Tank

The same geometry as used by Li et al. (2012) will be considered here. The tank is set up to be cylindrical with seven equidistant tubes imbedded in the composite. Each tube is 0.05 meters in diameter and each tube is far enough from the others that the heat transfer from a tube does not interfere with another. Therefore, each tube can be treated separately in the thermal analysis. The diameter of the circle that allows each tube to be thermally separate is 0.3 meters. Because of this, the diameter of the tank is assumed to be three times the length of the diameter of the thermal barrier so that the diameter of the tank is 0.9 meters.
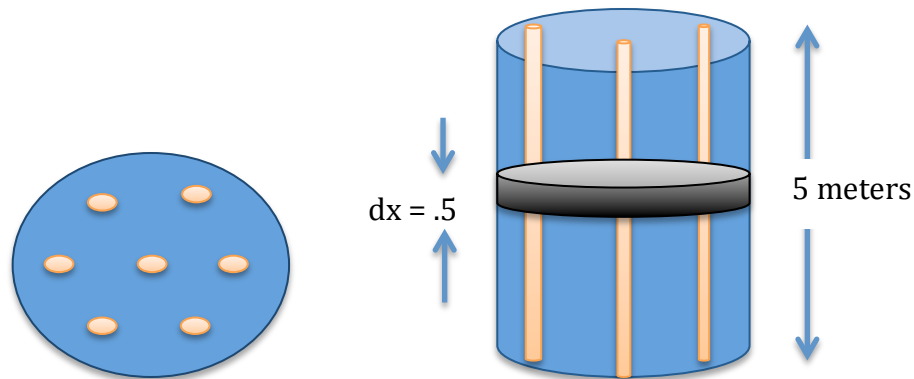

FIGURE 1: Geometry of storage tank based on Li et al. (2012)

Thermal Analysis

From Duffie and Beckman (2006), a simplified system can be created. Conduction is assumed to be infinite in order to simply the equations. Unfortunately,

14

using this form of analysis means that the difference in thermal conductivity

between the composites combinations is not considered. The following equations,

which consider the differences in heat capacity between the composites, are used:

$$\frac{\delta T_f}{\delta x} = \left(\frac{UP}{(\dot{m}C_p)_f}\right)(T - T_f) \tag{8}$$

$$\frac{\delta u}{\delta t} = \left(\frac{UP}{\rho A}\right)(T_f - T) \tag{9}$$

where:

$$u = \begin{cases} C_S(T_f - T) & if\ T < T^* \\ C_S(T^* - T_{ref}) + \chi\lambda & if\ T = T^* \\ C_S(T^* - T_{ref}) + \lambda + C_l(T - T^*) & if\ T > T^* \end{cases} \tag{9a}$$

In this set of equations, T_f is the temperature of the heat transfer fluid, T is

the temperature of the storage medium, U is the overall heat transfer coefficient, P is

the perimeter meeting between the storage medium and the heat transfer fluid, A is

the area between the storage medium and the heat transfer fluid, x is the distance

down the length of the storage tank, $\dot{m}$ is the mass flow rate of the heat transfer

fluid, λ is the latent heat of the salt in the composite, T^* is the melting temperature of

the storage medium, and T_{ref} is the temperature at which the internal energy is

assumed zero. For the purposes of this study, the equations can be simplified to the

following:

$$T_{f,2} = T_{f,1} + \Delta x\left[\left(\frac{UP}{(\dot{m}C_p)_f}\right)(T_{S,1} - T_{f,1})\right] \tag{10}$$

$$T_{S,2} = \begin{cases} T_{S,1} + \left[\frac{UP\Delta t}{\rho A C_S}(T_{f,1} - T_{S,1})\right] & if\ T_{S,2} > T_m > T_{S,1} \\ T_{S,1} + \left[\frac{UP\Delta t}{\rho A C_S}(T_{f,1} - T_{S,1}) - 0.8\lambda\right] & if\ not \end{cases} \tag{11}$$

For the purposes of this study, 80% of the latent heat (.8λ in the equation above) is used instead of the full latent heat of the salt, because each composite is 80% salt by weight.

However, since the system of calculation is by small changes in time and distance, the latent heat cannot just be subtracted because the temperature will realistically be unchanged for some time. Therefore, the equations must be altered farther with logical statements:

$$If\ T_{S,1} < T_m, T_{S,2} = \ T_{S,1} + \left[\frac{UP\Delta t}{\rho AC_S}\left(T_{f,1} - T_{S,1}\right)\right] \tag{12}$$

but:

$$If\ T_{S,2} > T_m, \quad T_{S,2} = T_m \tag{12a}$$

Of course, equation (12) is only accurate until the material under investigation takes in enough energy to convert all of the salt to liquid. Therefore, another condition is placed on the set of equations:

$$While\ T_{S,2} = T_m, \quad u = \frac{UP\Delta t}{\rho AC_S}\left(T_{f,1} - T_{S,1}\right) \tag{13}$$

$$After\ the\ sum\ of\ all\ u\ equals\ 0.8\lambda,\ T_{S,2} = \ T_{S,1} + \left[\frac{UP\Delta t}{\rho AC_S}\left(T_{f,1} - T_{S,1}\right)\right] \tag{14}$$

This set of logical expressions and equations accurately follows the temperature profile for each chunk of the tank. Each following chunk uses the output fluid temperature of the preceding chunk as the input fluid temperature and the initial storage media temperature for each chunk is assumed to be the same.

Cost Analysis

The cost analysis was done using the equations from Ren et al. (2011) and Wu et al. (2011):

$$C = \frac{P}{Q} \qquad (15)$$

where P is the overall price of the composite per unit of mass (\$/kg) and Q is the energy stored per mass divided by 3600 (kWh/kg). The energy stored in the material per unit of mass can be calculated using equation (9a) from above for u, and therefore, Q can be written as follows:

$$Q = \frac{u}{3600} \qquad (16)$$

Chapter Three

Material Thermophysical Properties and Costs

This section contains the information that will be input into the analysis equations in order to attain the results in Chapter Four. Within the next several graphs, jumps and discontinuities exist in the data due to the piecing together of data from various articles. Properties were interpolated between sets of data and extrapolated out from available data. Cost and thermophysical properties for each individual material follow.

Thermal Conductivity

Ceramics and Graphite

The individual materials' thermal conductivities are shown in Figures 2a and 2b. The thermal conductivity of the aluminum oxide and the magnesium oxide are clearly similar, while the zirconium oxide has much lower thermal conductivities. The thermal conductivity of the graphite is clearly much higher than that of the ceramics. Due to this fact, the ceramics are practically invisible in Figure 2a, and are therefore shown again in Figure 2b without graphite so that the differences between the ceramics can be seen. The thermal conductivities were estimated based on info from Zabolotskii (2011), Yaws (2009).
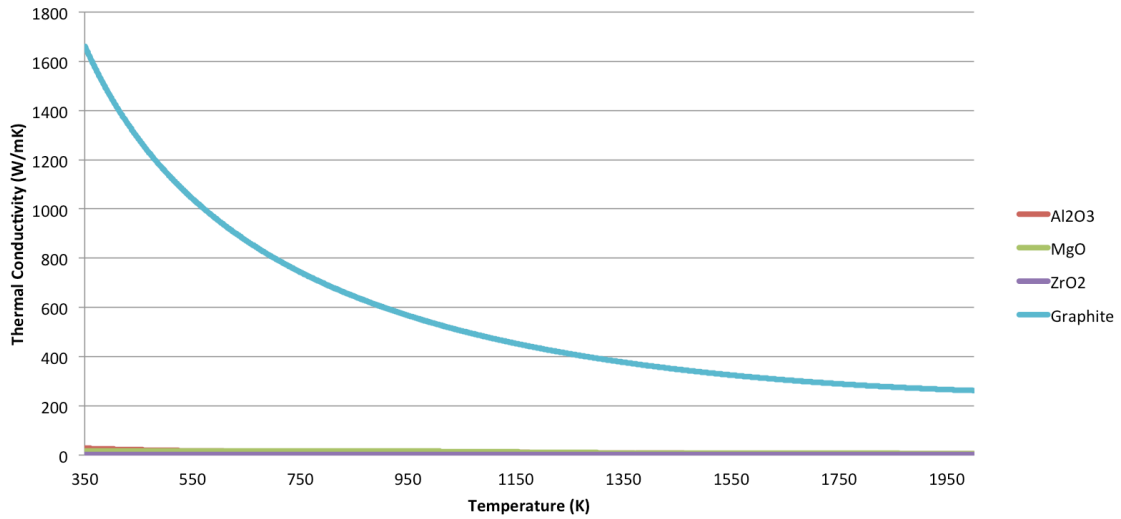
18

FIGURE 2a: Thermal conductivity of the ceramics under investigation and graphite
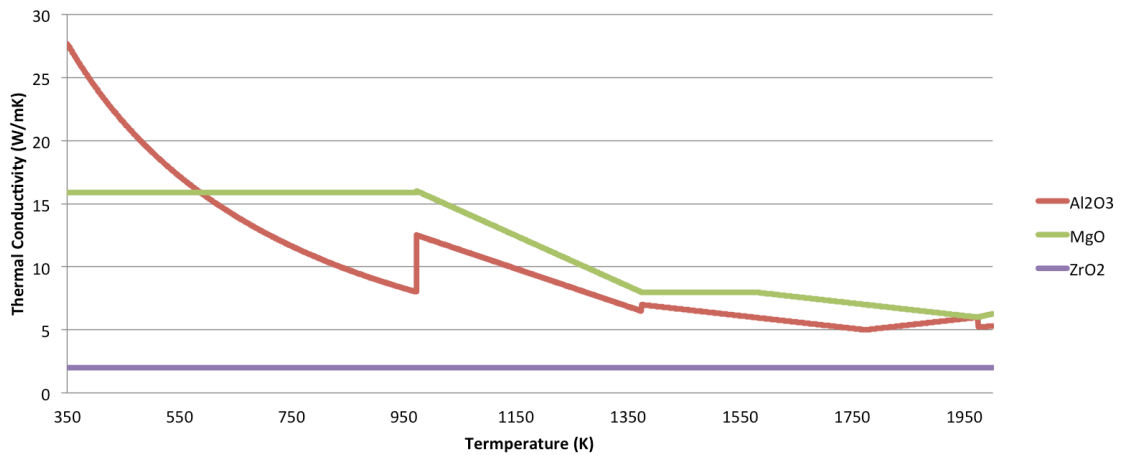

FIGURE 2b: Thermal conductivity of only the ceramics under investigation

Salts

The thermal conductivity of the salts being investigated is shown in Figure 3. The carbonate salts (Li_2CO_3 and Na_2CO_3) have higher thermal conductivity values than the other salts, but the reference for each was only available in the range of 1100-1300K. For the rest of the temperature range, the thermal conductivity was assumed constant on either end of the available values. The nitrate salts ($NaNO_3$,

19

LiNO$_3$, and KNO$_3$) had available data at lower temperatures, which leveled off around 700K. For the purposes of this project, the thermal conductivity after leveling off was assumed to stay constant for the rest of the temperature range. The thermal conductivity of the salts were found in Bauer et al. (2012), Yaws (2009), Taha (1991), and Kenisarin (2010).
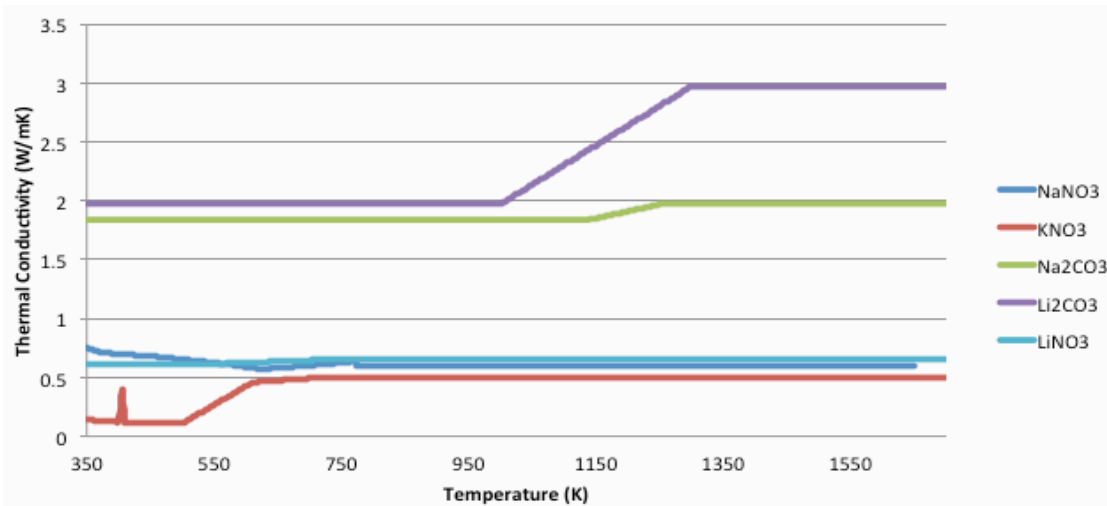

FIGURE 3: Thermal Conductivity of Salts Under Investigation

Specific Heat Capacity

Ceramics and Graphite

The specific heat of the ceramics and graphite are shown in Figure 4. The graphite has a higher heat capacity than the ceramics being investigated. Up until around 900K, the magnesia and the alumina follow a similar pattern. Above 900K, the magnesia's specific heat capacity becomes much higher than the specific heat capacity of the alumina. Specific data were found for each of the ceramics until about 900K. The data for NaNO$_3$ were extrapolated from the end point of the available data to remain constant for the remainder of the temperature range.

Above around 1300K, the same was done for magnesia. The alumina and graphite datasets were available for an extreme temperature range and, therefore, there was no need to interpolate or extrapolate. The heat capacity for the ceramics and graphite were found in Zabolotskii (2011), and Graphite and Composites (website).

Salts

Figure 5 contains the heat capacity data for each of the salts under investigation. The heat capacity for the salts were not available over all temperatures, so the heat capacity was assumed to stay constant after the temperature at which the data was no longer available. The heat capacity for sodium nitrate increases abruptly at its melting temperature based on the ouput data in Bauer et al. (2012), but this increase could be due to involvement of the latent heat in this assessment. Since this cannot be definitively found as true, the data is assumed accurate with the sudden increase. The heat capacity of the salts were found in Bauer et al. (2012), Kenisarin (2010), Gokon et al. (2009) and Kourkova et al. (2007).
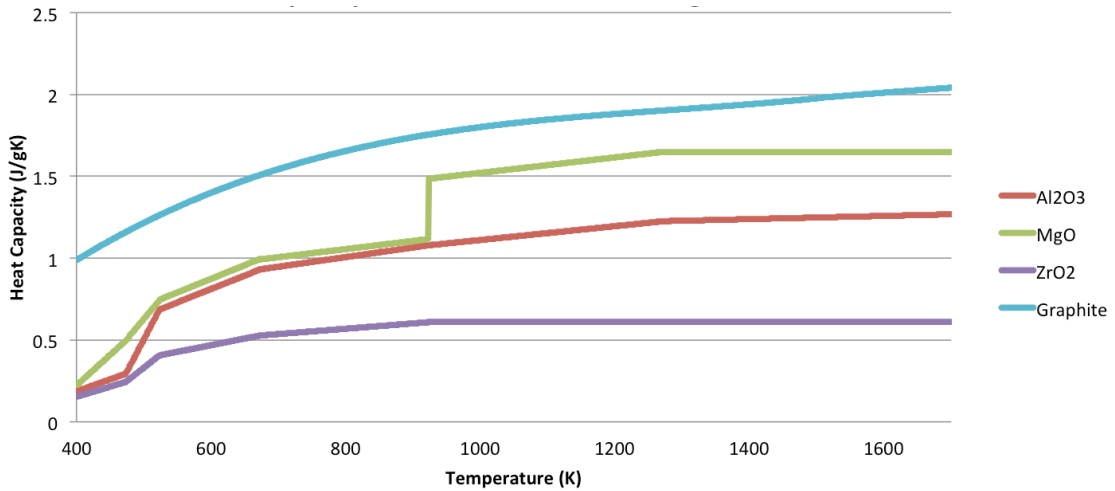
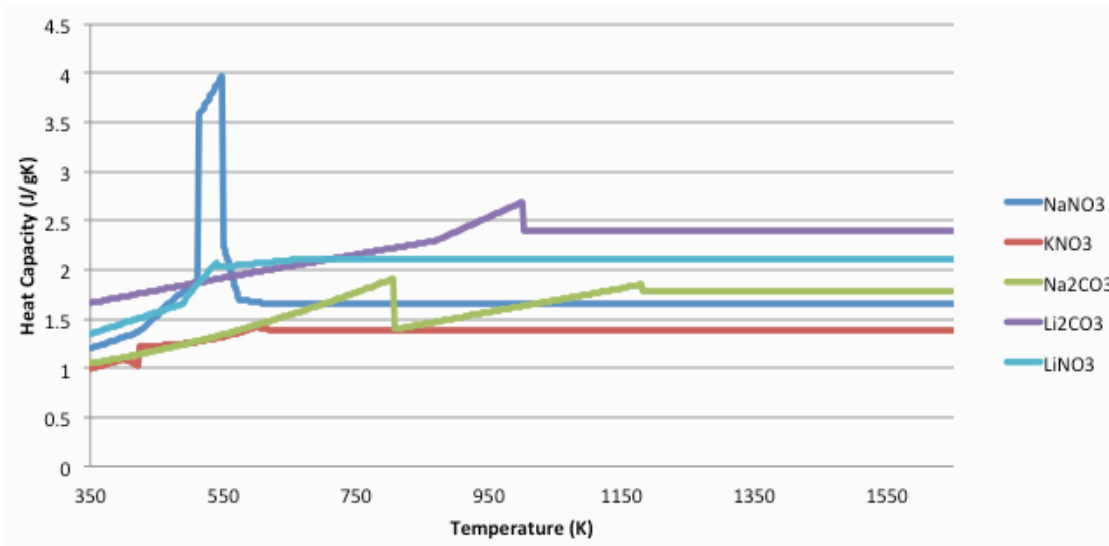*Figure 4*: Heat capacity of the ceramics under investigation and graphite

Figure 5: Heat Capacity of Salts Under Investigation

Thermal Analysis

Since the system is assumed to be a high temperature system, a heat transfer fluid is needed that will not boil at these temperatures or solidify if the temperature drops. The heat transfer fluid used for this assessment is a combination of LiF, NaF, and KF, popularly called FLiNaK. This material has been investigated for decades

and has been studied for use in high temperature Brayton cycle systems. For this material, the density, heat capacity and heat transfer coefficient are:

$$\rho_{FLiNaK}\left(\frac{kg}{m^3}\right) = 976.13 - 1.063(T_f - 273) \qquad (17)$$

$$C_{P,FLiNaK}\left(\frac{J}{kgK}\right) = 2530 - 0.730(T_f - 273) \qquad (18)$$

$$U\left(\frac{W}{m^2K}\right) = 14000 \qquad (19)$$

The density (ρ_{FLiNaK}) and heat capacity ($C_{P,FLiNaK}$) were found in Holcomb et al. (2010) and the overall heat transfer coefficient (U) was estimated from Hoffman et al. (1955). For the thermal analysis, the storage material is assumed to be at an initial temperature of 500K and the heat transfer fluid is assumed to be 1300K. The geometry of the tank is described above to be 5 meters long and 0.9 meters in diameter, with seven equally spaced tubes embedded into the storage material of diameter 0.05 meters. The latent heat and melting temperature needed for each salt was found in Kenisarin (2010). The density of each material for the analysis was found in Bauer et al. (2012), 'About Zirconia' (website), Janz (1988), 'Material: Aluminum Oxide' (website), 'Graphite Powder' (website), Zabolotskii (2011).

Cost Analysis

The cost analysis for each of the combinations was done with the following price per kg in Table 1 as ascertained from Fisher Scientific (website).

Table 1: Cost per unit mass of each material under investigation

Material	Price per mass ($/kg)
Alumina	$67.68
Magnesia	$136.36
Zirconia	$168.34
Graphite	$290.30
Sodium Nitrate	$97.64
Potassium Nitrate	$89.41
Sodium Carbonate	$65.02
Lithium Carbonate	$160.59
Lithium Nitrate	$137.29

The

energy stored was calculated assuming a temperature change from 573K to 2273K,

allowing for each of the materials to be under the same conditions and each of the

melting temperatures to be in the temperature range under investigation. Also, the

range of operating temperatures for a power tower is 300°C-2000°C so that the high

and low temperatures that the storage material experience are the high and low

temperatures for the system.

Chapter Four

Results

By inputting the cost and thermophysical properties from Chapter Three into the analysis equations in Chapter Two, the following output data were created.

Thermal Conductivity

Each composite under investigation is shown below in Figures 6a-e. The charts are separated by the ceramic being used. Each chart has extremely similar shape, showing that the salt mostly determines the behavior of the composite overall. However, the range of values seen for the thermal conductivity varies between the ceramic types. As seen in the previous charts for thermal conductivity of the ceramics/graphite, the graphite composites tend to have higher thermal conductivity values than the other composites. The alumina and magnesia composites have extremely similar thermal conductivity values, as seen below, while the zirconia has noticeably lower values. These results mirror the properties reviewed in Figure 2.

Figures 6a, 6b, and 6c all have the same order of composites, where the highest thermal conductivity is in the graphite composite, followed by the magnesia composite and alumina composite, which are almost exactly the same, then the zirconia composite, and lastly, the salt alone. These figures are the nitrate salts, which all had similar thermal conductivities. Figure 6b of potassium nitrate and the composites made with potassium nitrate contains a blip at a low temperature. This jump looks big on this scale, but occurs based on the input data from Taha (1981).
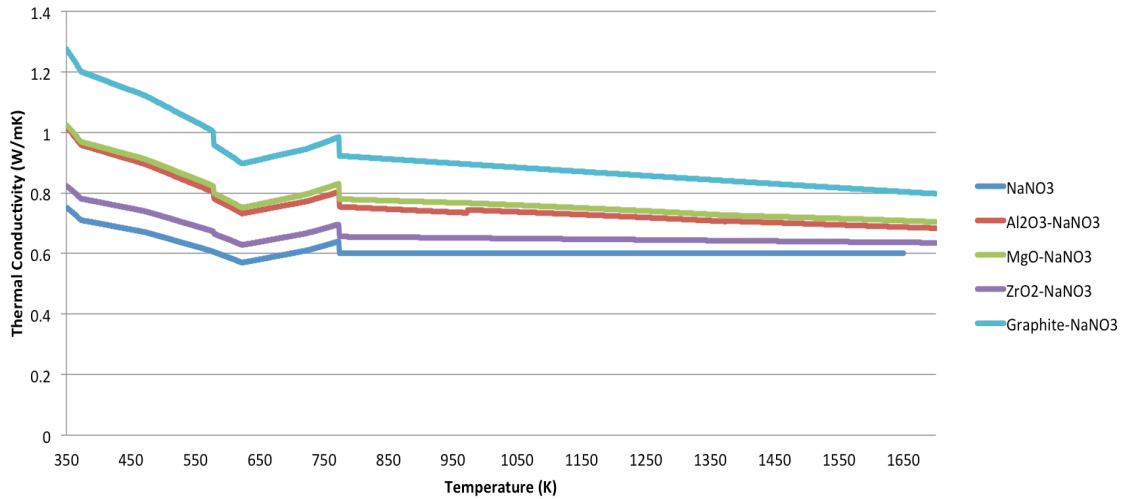
FIGURE 6a: Thermal conductivity of sodium nitrate and effective thermal conductivity of composites made with sodium nitrate
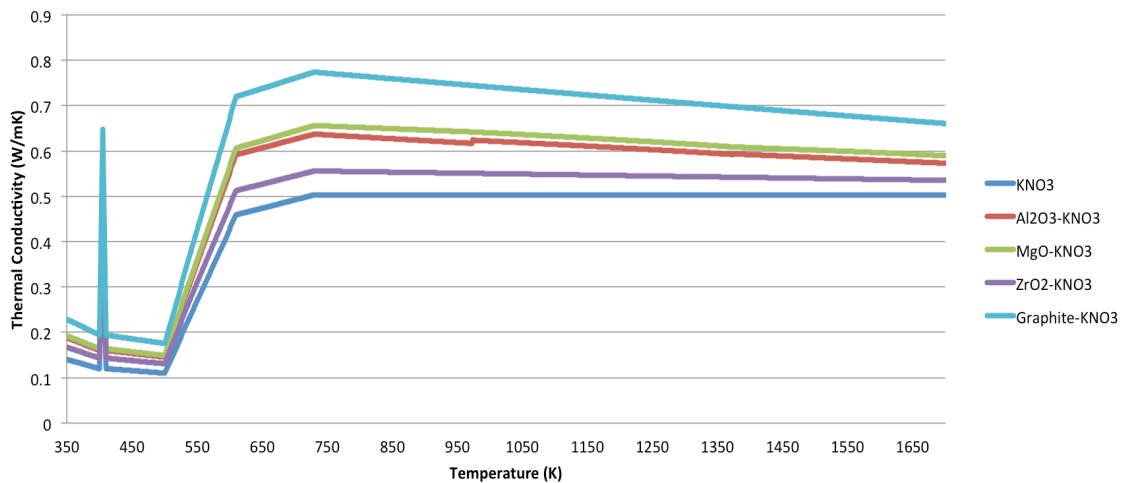

FIGURE 6b: Thermal conductivity of potassium nitrate and effective thermal conductivity of composites made with potassium nitrate

Figures 6d and 6e are the carbonate salts and the composites made with the carbonate salts. In these two graphs, the zirconia composites cannot be seen as different from the salts alone. This is because the carbonate salts have higher thermal conductivity values than the nitrate salts and the added zirconia is not able to improve the thermal conductivity of the carbonate salts.
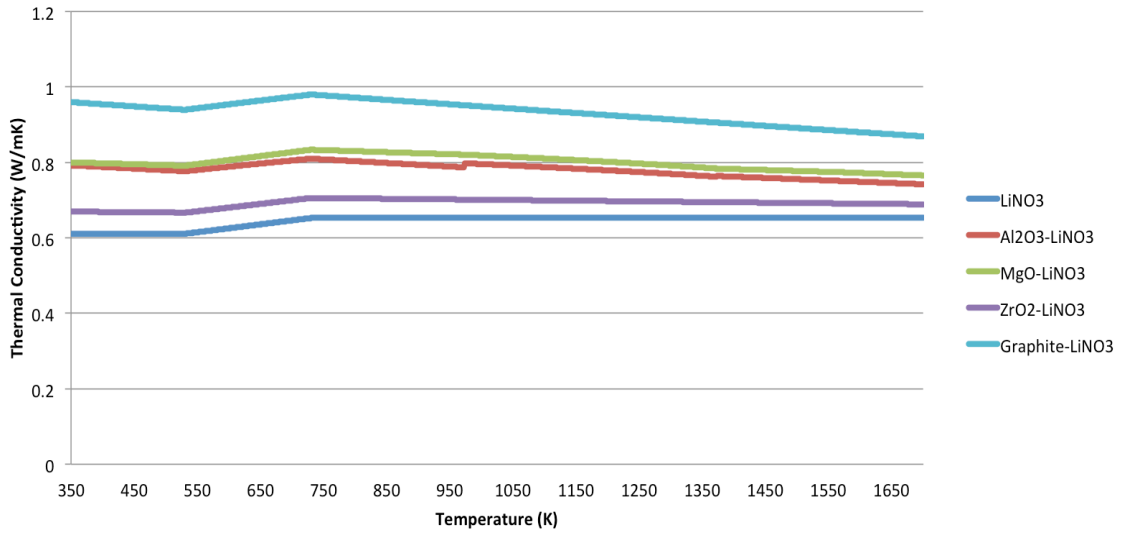
26

FIGURE 6c: Thermal conductivity of lithium nitrate and effective thermal conductivity of composites made with lithium nitrate
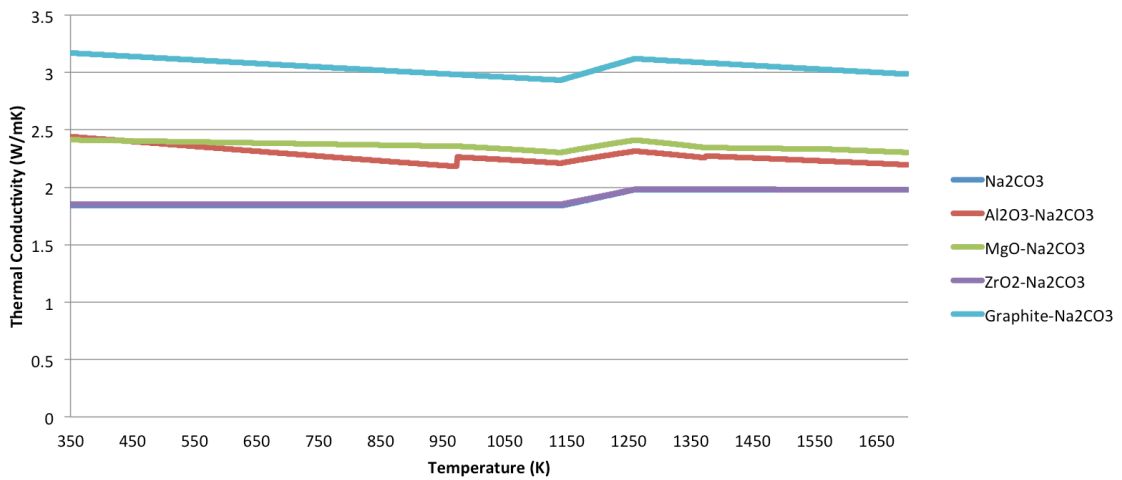

FIGURE 6d: Thermal conductivity of sodium carbonate and effective thermal conductivity of composites made with sodium carbonate

Overall, the thermal conductivity graphs have the same organization, although

different salts have been used and the actual pattern within the graphs is different.
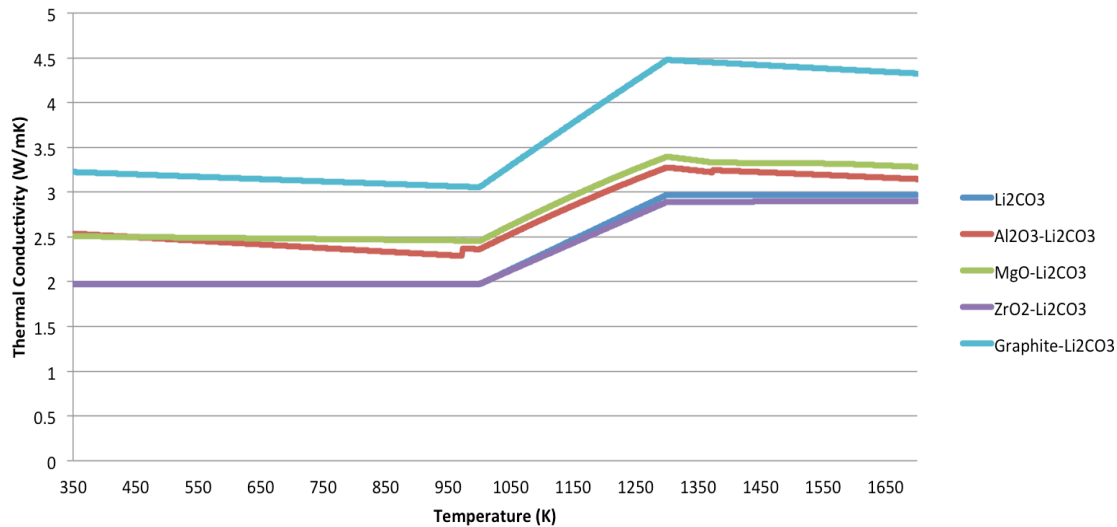
FIGURE 6e: Thermal conductivity of lithium carbonate and effective thermal conductivity of composites made with lithium carbonate

Specific Heat Capacity

Figures 7a-e contain the effective heat capacities for each composite combination. Again, because the composite would be comprised mostly of the salt, the behavior of the heat capacity over the various temperatures is seen to be mostly determined by the salt's heat capacity. The actual numbers vary due to the contribution of the ceramic or graphite. The effective heat capacity for the alumina and magnesia composites are almost identical, while the graphite composites have a slightly higher effective heat capacity and the zirconia composites have a slightly lower heat capacity than the alumina and magnesia composites.

Figure 7a contains the heat capacity for the sodium nitrate and the composites made with sodium nitrate. For the most part, the sodium nitrate's heat capacity is actually higher than the other materials in this graph, but at higher temperatures, the heat capacity of the composite with graphite and sodium nitrate

does become higher than the salt alone. The zirconia and sodium nitrate composite clearly consistently has the lowest heat capacity of the sodium nitrate composites.

Figure 7b shows the heat capacity for the potassium nitrate and the composites made with potassium nitrate. In this graph, the heat capacity of potassium nitrate is not consistently higher than the potassium nitrate composite. The heat capacity of the graphite and potassium nitrate composite is about the same as the potassium nitrate until about 600K. Above 600K, the heat capacity of the graphite and potassium nitrate is higher than the heat capacity of the potassium nitrate itself. The composite with zirconia and potassium nitrate has the lowest heat capacity overall.
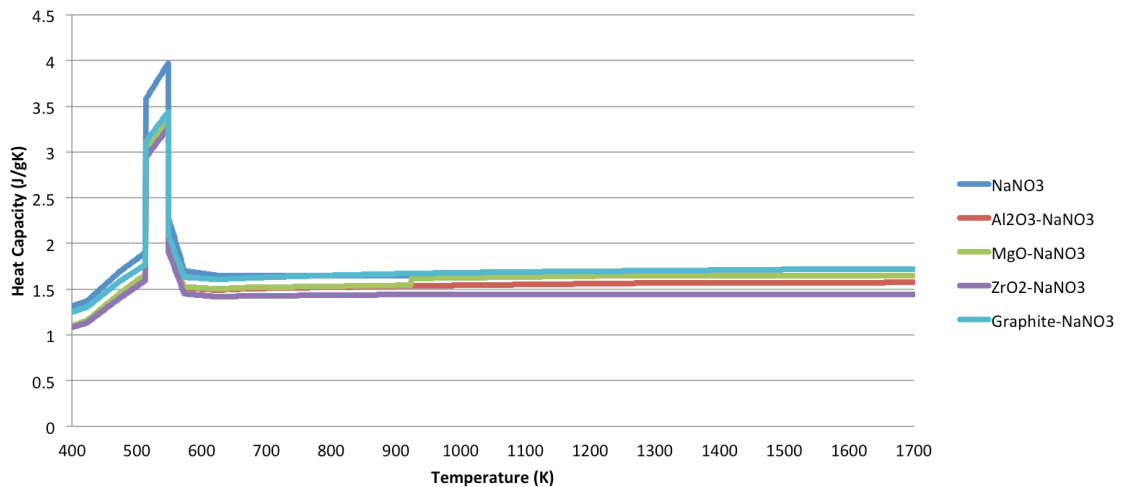

FIGURE 7a: Heat capacity of sodium nitrate and effective heat capacity of composites made with sodium nitrate
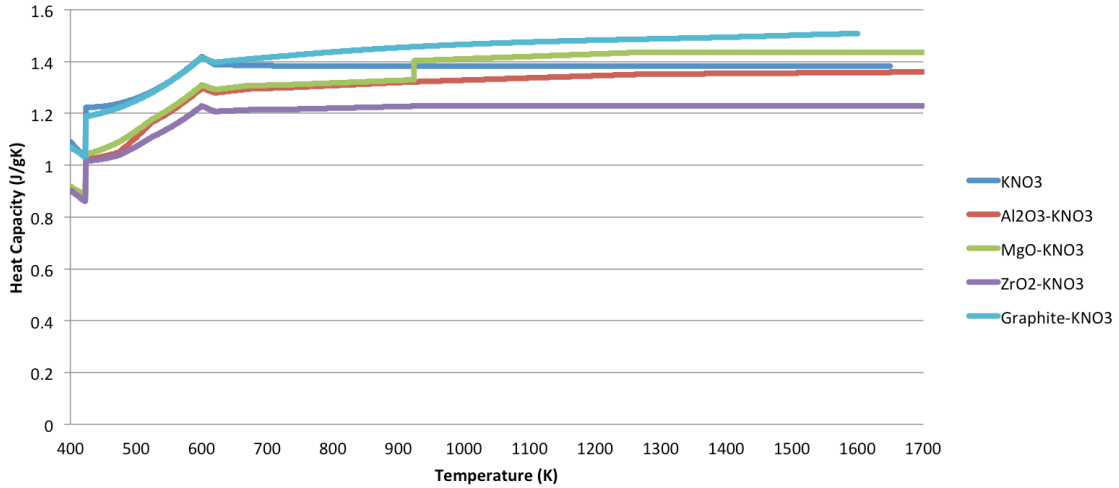
FIGURE 7b: Heat capacity of potassium nitrate and effective heat capacity of composites made with potassium nitrate

Figure 7c shows the heat capacity of lithium nitrate and the composites made with lithium nitrate. The lithium nitrate alone has the highest heat capacity, but not by much. The composite made of zirconia and lithium nitrate is the lowest heat capacity of this graph. As usual, the heat capacity of the composites with the alumina and the magnesia are very similar. Overall, the heat capacities are all very similar.
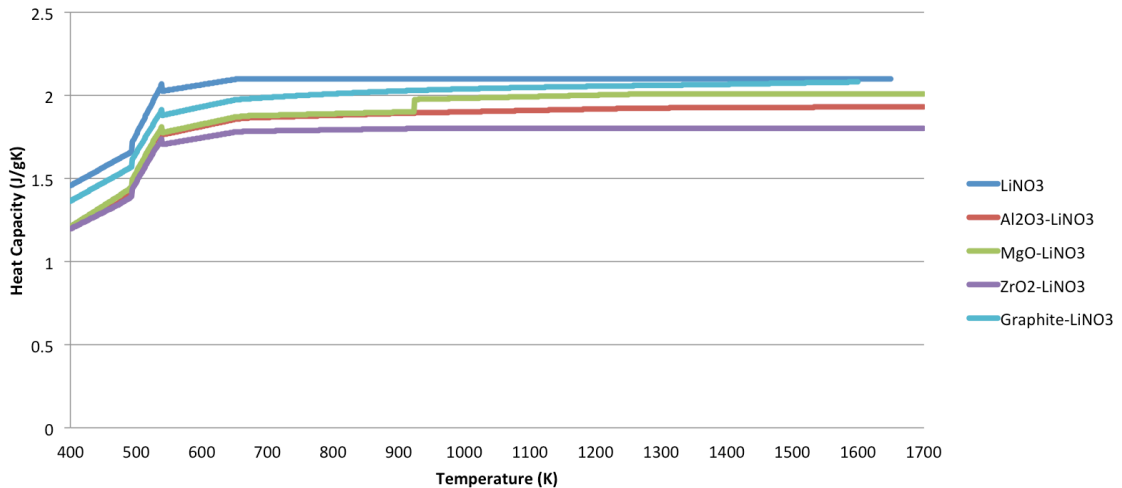

FIGURE 7c: Heat capacity of lithium nitrate and effective heat capacity of lithium-nitrate-based composites

30

Figure 7d contains the heat capacity of sodium carbonate and the composites made of sodium carbonate. The composite of sodium carbonate and zirconia is the lowest of the sodium carbonate composites. The sodium carbonate by itself is not consistently the highest heat capacity. The heat capacity of the composite of sodium carbonate and graphite is higher than the sodium carbonate alone over some temperature ranges. The heat capacity of the alumina and magnesia composites are extremely similar.
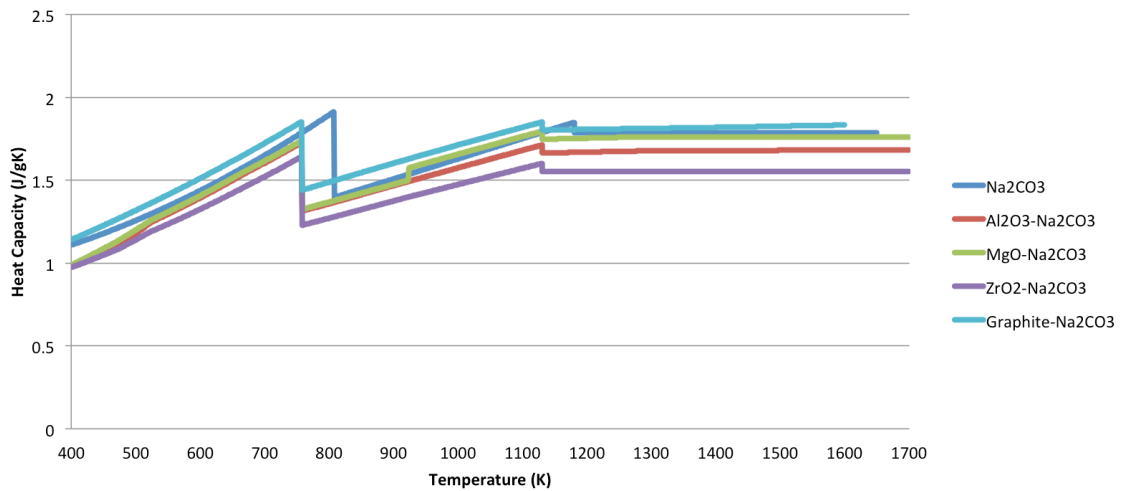

FIGURE 7d: Heat capacity of sodium carbonate and effective heat capacity of sodium-carbonate-based composites

Figure 7e shows the heat capacity for lithium carbonate and the composites made of lithium carbonate. Lithium carbonate alone has the highest heat capacity, followed by the graphite composite, the magnesia composite, the alumina composite, and the zirconia composite. Again, all of these are extremely similar, so while differences exist between the composites, they are slight differences.
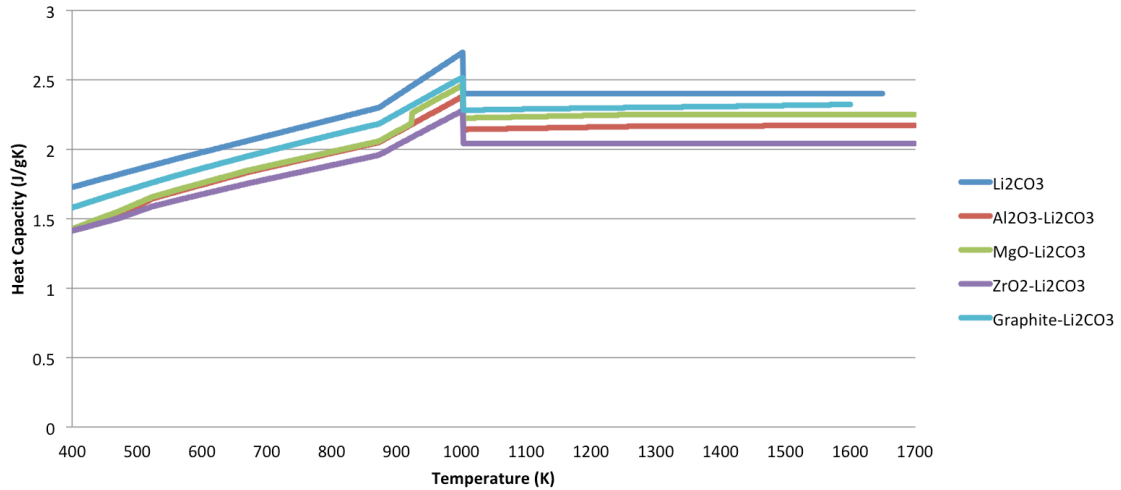
31

FIGURE 7e: Heat capacity of lithium carbonate and effective heat capacity of lithium-carbonate-based composites

Thermal Analysis

For comparison, the first set of data is for each salt by itself. Figure 8a and 8b show the temperature over time of the first half of a meter and the last half of a meter of the tank.
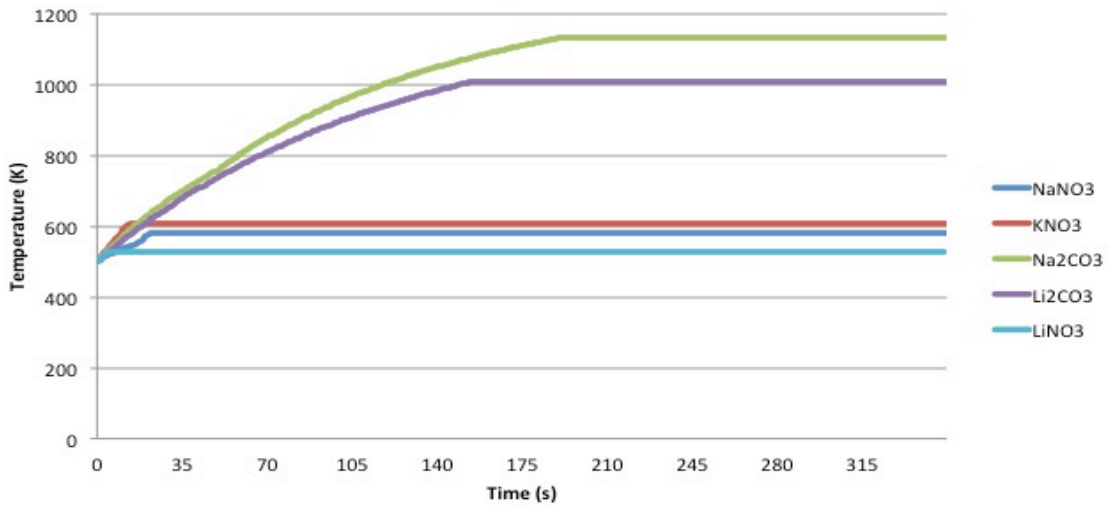

FIGURE 8a: Thermal Analysis of the Salts Under Investigation in the first half-meter of the tank
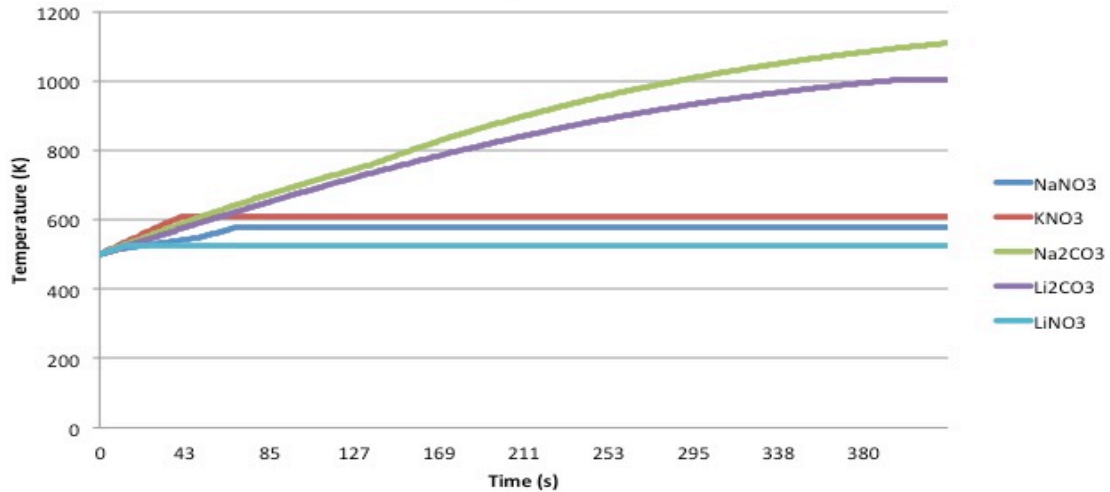
FIGURE 8b: Thermal Analysis of Salts Under Investigation in the last half-meter

These graphs are only the first few minutes after the heat transfer fluid begins to enter the storage tank. In the first half of a meter, each of the salts begins to change phase within the first several minutes. The temperature clearly levels off at each salt's melting temperature in the first half-meter, but not the last half-meter. In the last half-meter, all but the sodium carbonate reaches the melting temperature within the first five or six minutes

To more clearly show where in the tank the analysis is being conducted, Figure 9 shows the analysis zones. The cylinder on the left highlights the first half of a meter of the tank where the hot heat transfer fluid enters the tank. The cylinder on the left highlights the last half of a meter of the tank where the cold heat transfer fluid leaves the tank. Each of the following graphs for the various composites is for either one of these analysis zones.
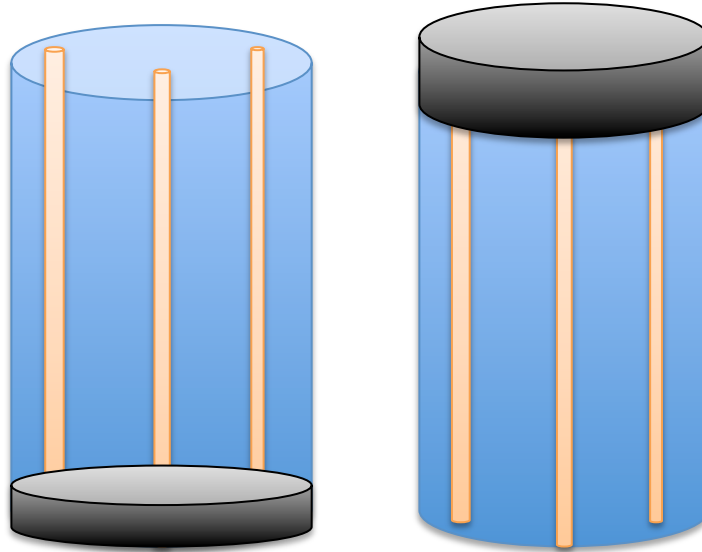
FIGURE 9: On the left, the first half of a meter is depicted where the hot heat transfer fluid enters; on the right, the last half of a meter is depicted where the cold heat transfer fluid leaves

The behavior of the temperature in Figures 10a and 10b are almost identical to each other. These graphs are of the temperature change in both the composites made with sodium nitrate, and for comparison, sodium nitrate itself. Figure 10a is of the first half of a meter as the hot heat transfer fluid enters the storage material. Figure 10b is of the last half of a meter of the storage tank as the cold heat transfer fluid leaves the tank. While the behavior of the temperature is the same, the time element is different. It takes about three times longer for the end of the tank to reach the melting temperature than the beginning of the tank. The sodium nitrate temperature is consistently lower than any composite temperature, while the graphite and sodium nitrate composite is consistently higher in temperature than the other materials. The composites made with the ceramics and sodium nitrate are all along the same trajectory with only minor differences. This analysis is made

without conduction though, so the temperature of the storage material would likely

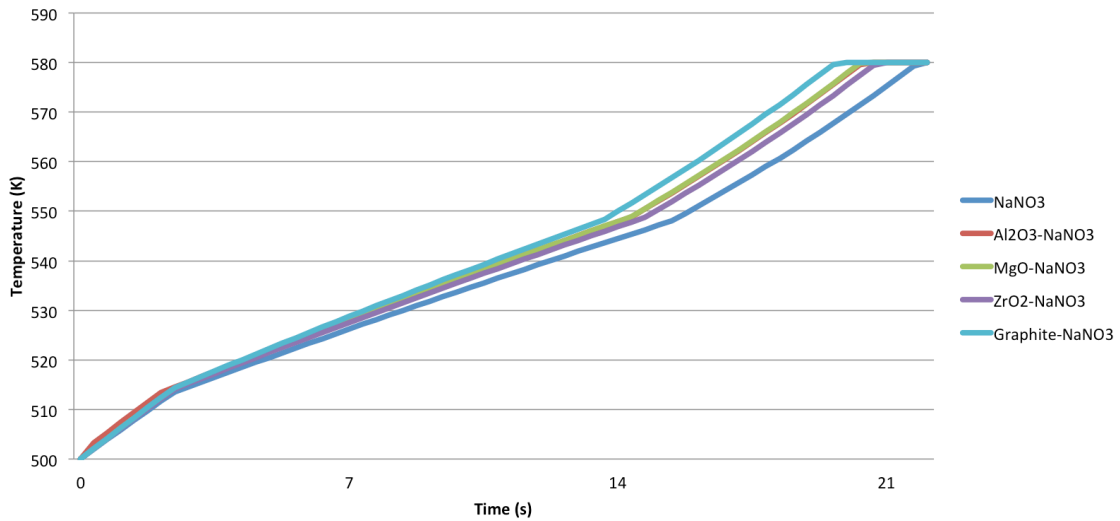change greatly with conduction used, especially the graphite composite.

FIGURE 10a: Temperature change over time until the melting temperature is reached for sodium nitrate and the composites made with sodium nitrate in the first half of a meter of the storage tank

FIGURE 10b: Temperature change over time until the melting temperature for sodium nitrate and the composites made with sodium nitrate for the last half of a meter in the storage tank

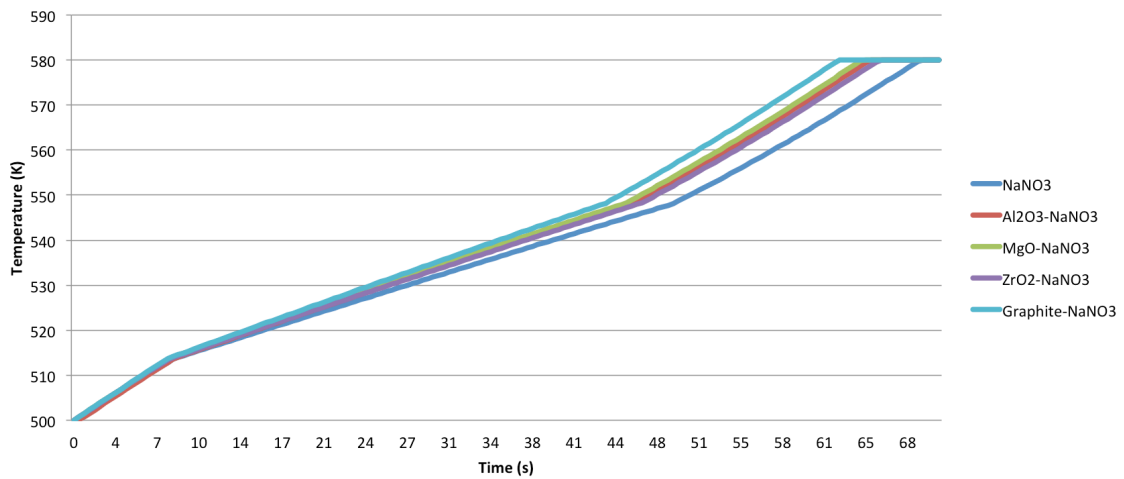Figures 11a and 11b are the temperature changes over time in the same area

of the tank as the previous two sets of graphs. The behavior of the temperature of

time is clearly determined again by the salt, but in this graph, the different materials

35

are indistinguishable. Therefore, these materials, because of their similar properties, will react similarly when heat is added.

FIGURE 11a: Temperature change over time of potassium nitrate and the composites made with potassium nitrate until the melting temperature is reached in the first half of a meter of the storage tank
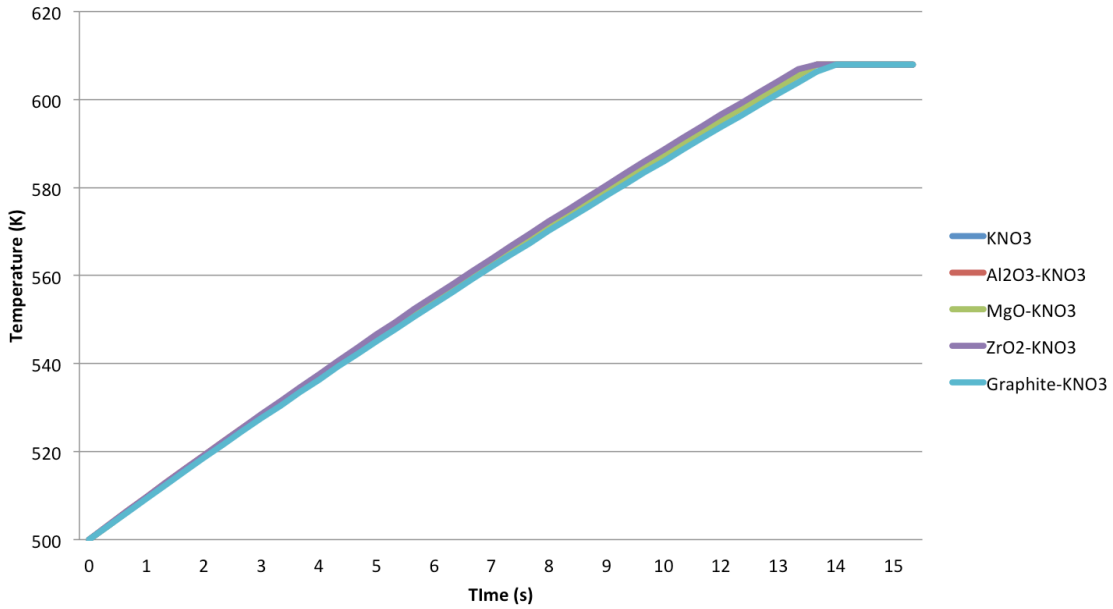

FIGURE 11b: Temperature change over time of potassium nitrate and the composites made with potassium nitrate until the melting temperature is reached in the last half of a meter of the storage tank

Figures 12a and 12b show the temperature change over time in first and last half of a meter of the storage tank when the storage material is lithium nitrate or any of the composites made with lithium nitrate. The temperature of the lithium nitrate is slightly less than the others over most of the graph in Figure 12a.

FIGURE 12a: Temperature change over time of lithium nitrate and composites made with lithium nitrate until the melting temperature is reached in the first half of a meter of the tank
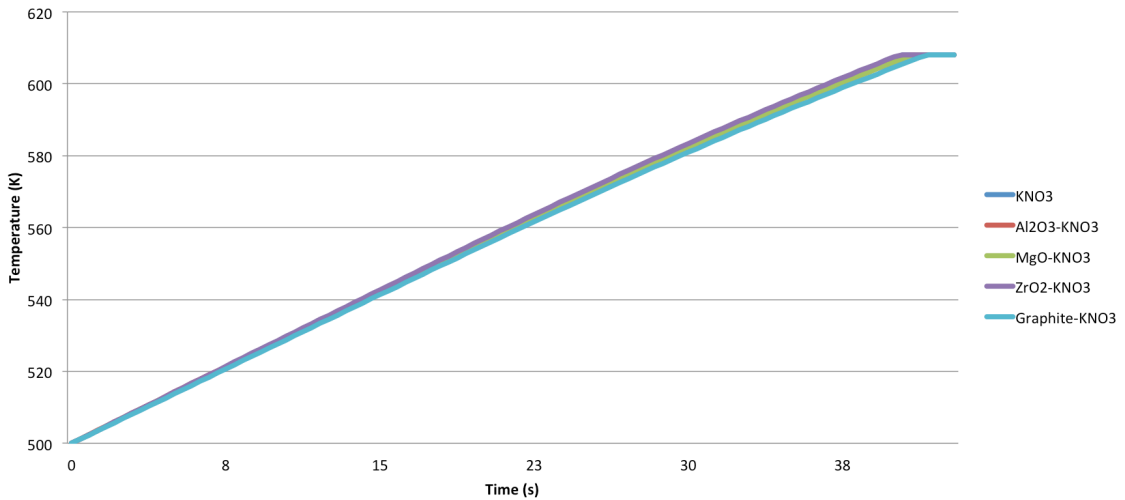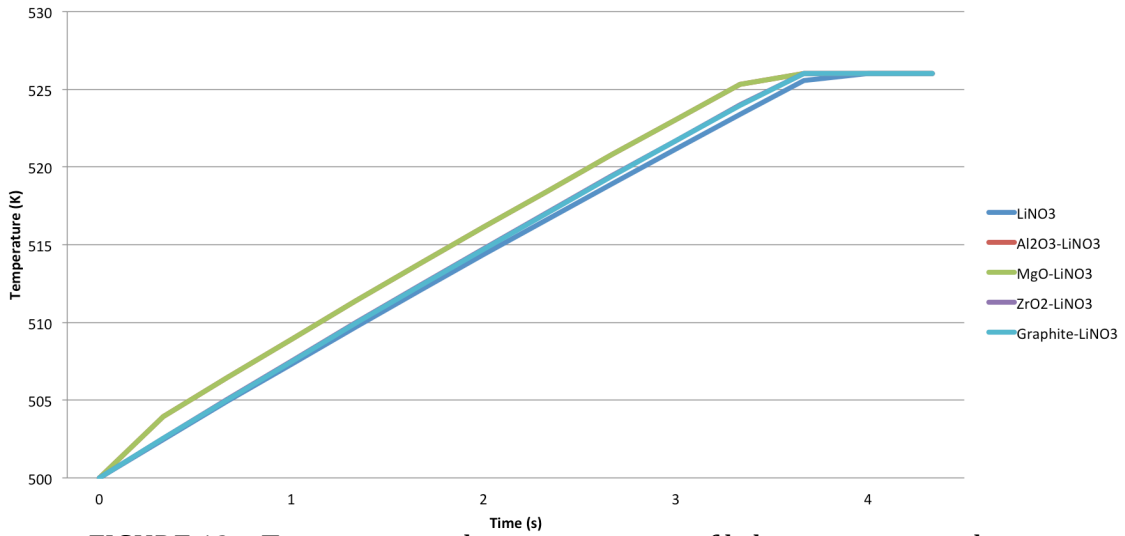

FIGURE 12b: Temperature change over time of lithium nitrate and composites made with lithium nitrate until the melting temperature is reached in the last half of a meter of the tank

Figures 13a and 13b show the temperature change in the same areas of the tank as above, but with sodium carbonate and the composites made with sodium carbonate as the storage medium. Unlike the previous graphs, the lines for the sodium carbonate and the composites made of sodium carbonate are indistinguishable. They do vary from each other, but not enough to see at this scale.

FIGURE 13a: Temperature change over time of sodium carbonate and composites made with sodium carbonate until the melting temperature is reached in the first half of a meter of the tank
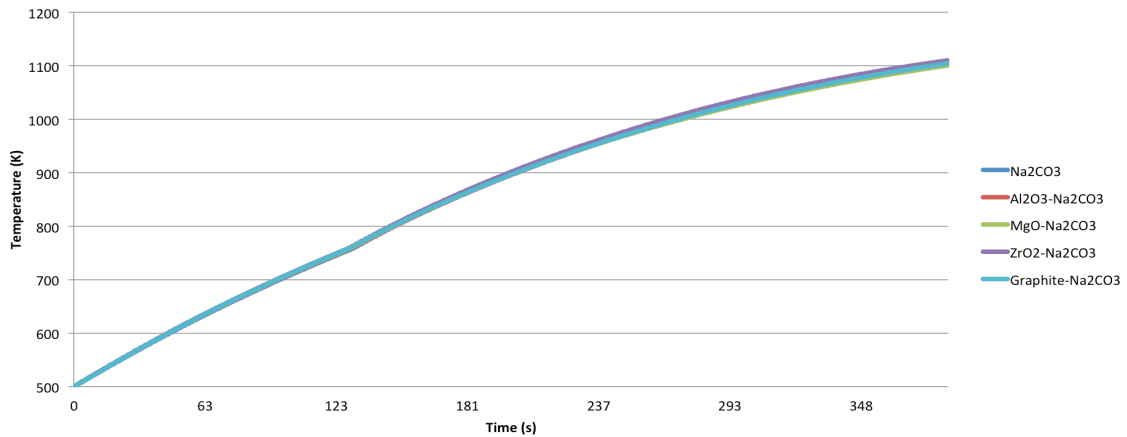
FIGURE 13b: Temperature change over time of sodium carbonate and composites made with sodium carbonate in the last half of a meter of the tank

Figures 14a and 14b are the last set of graphs concerning the temperature over time in the tank. These show the temperature over time for lithium carbonate and the composites made with lithium nitrate.

FIGURE 14a: Temperature change over time of lithium carbonate and composites made with lithium carbonate until the melting temperature is reached in the first half of a meter in the tank
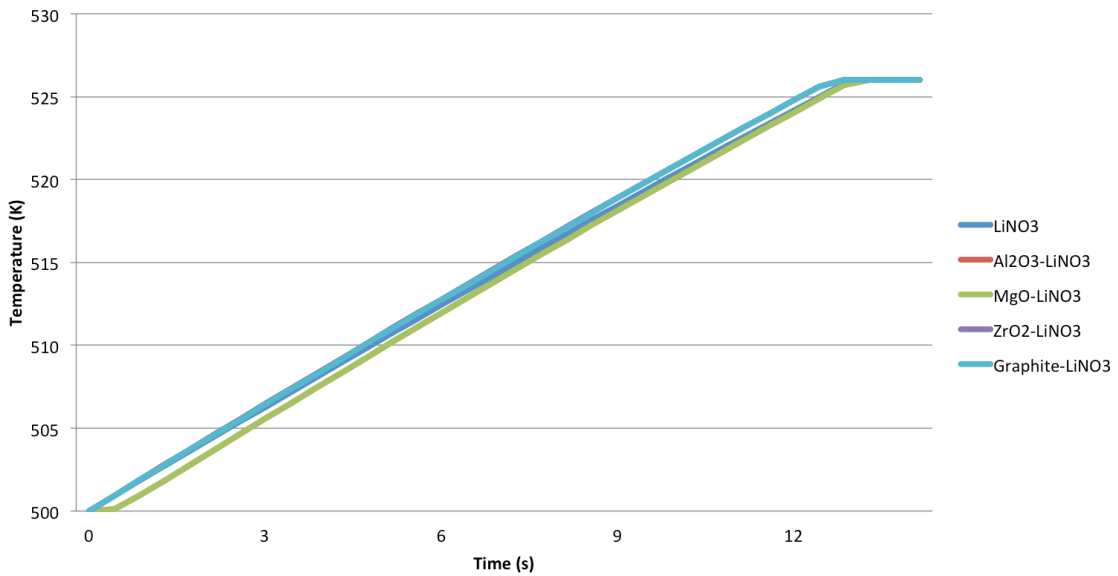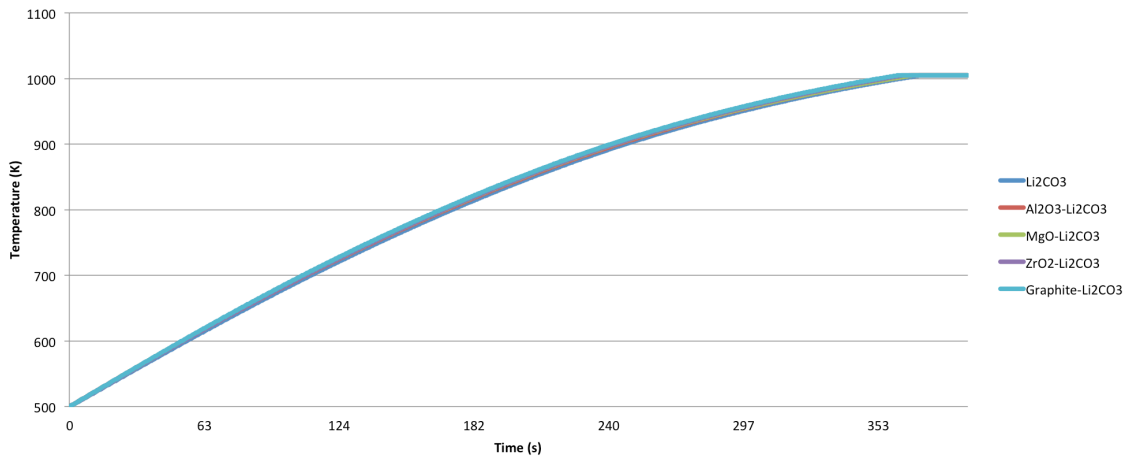

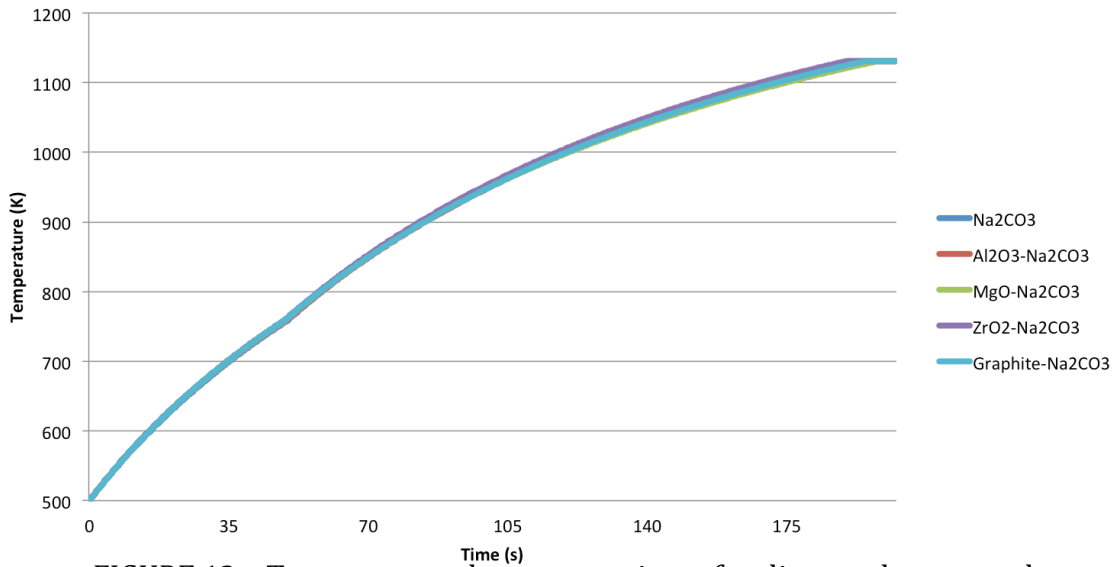*FIGURE 14b*: Temperature change over time of lithium carbonate and composites made with lithium carbonate until the melting temperature is reached in the last half of a meter in the tank
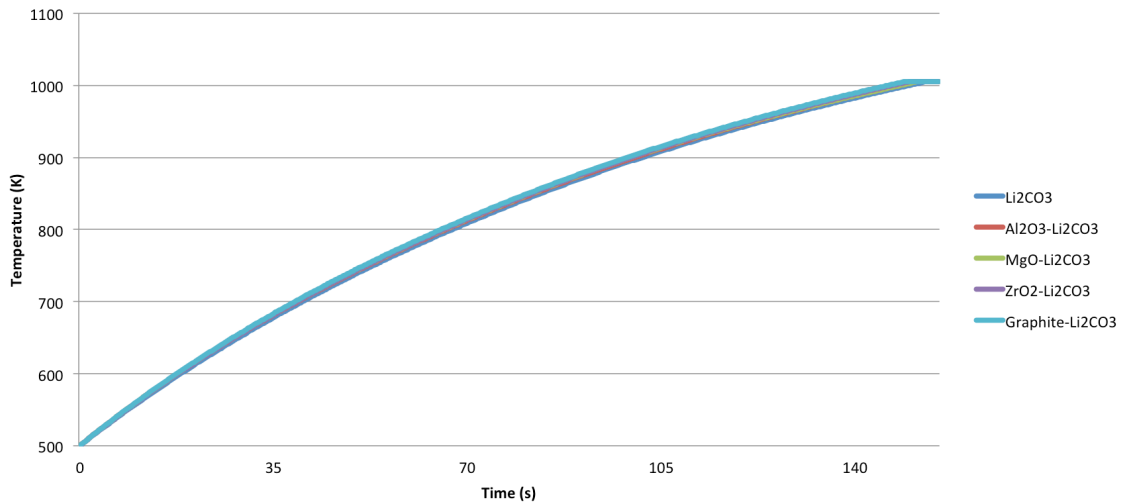
After seeing the similarity between the last several sets of graphs, the ceramic clearly does not affect the heat capacity of the salt. Graphite had drastically different thermal properties from the ceramics, but in this analysis, only convection was considered, so the thermal conductivity of the composites was not considered. Though the heat capacity of graphite was higher than the other ceramics, the graphite-based composites do not have a heat capacity much different from the salt.

Cost Analysis

Using equations (15) and (16) from above, the cost per kilowatt-hour is calculated for each composite (Table 2). Equation (16) showed how the storable energy in kWh_t per kilogram can be calculated using the internal energy of each material assuming a temperature range of 573-2273K based on the operating temperature of a solar tower (Barlev, 2011). Equation (15) calculated the cost in Table 2 by dividing the price of each composite per kilogram by the storage energy in kWh_t per kilogram. Therefore, the cost in Table 2 is simply the cost per storage kWh_t and does not take into account the other necessary parts of the system or the amounts that the power would be sold for over time.

Table 2: Cost of Composites per kWh_t

Composite	Cost ($/kWh)
Al2O3-NaNO3	$117.52
Al2O3-KNO3	$129.06
Al2O3-Na2CO3	$79.03
Al2O3-Li2CO3	$124.90
Al2O3-LiNO3	$124.27
MgO-NaNO3	$128.75
MgO-KNO3	$141.60
MgO-Na2CO3	$91.34
MgO-Li2CO3	$132.48
MgO-LiNO3	$132.93
ZrO2-NaNO3	$155.22
ZrO2-KNO3	$175.50
ZrO2-Na2CO3	$111.32
ZrO2-Li2CO3	$150.51
ZrO2-LiNO3	$153.80
Graphite-NaNO3	$160.85
Graphite-KNO3	$178.53
Graphite-Na2CO3	$122.83
Graphite-Li2CO3	$154.96
Graphite-LiNO3	$158.47

Based on the criteria for this calculation, the salt-ceramic of alumina and sodium carbonate is the most cost-effective composite that was analyzed at $79.03/kWh. The survey work of the Nevadan energy utilities from the Experimental Program to Stimulate Competitive Research (EPSCoR) grant did not have a large amount of data returned. However, one respondent requested that any storage medium cost them less than $0.06/kWh. This type of kilowatt-hour would be electric and the calculation above would be a thermal version of kilowatt-hours and therefore, these numbers are not comparable. However, the price requested from the energy utility is so low that we can expect that the cost of the composite materials would not be close to the requested price. Therefore, the salt-ceramic composite system would be

better utilized by a large corporation or even a large utility and not the small

utilities that are seen throughout Nevada.

Chapter Five

Conclusions and Recommended Future Work

When simply looking at the effective thermal properties of each composite, the composites made up graphite and lithium carbonate and graphite and sodium carbonate have the highest thermal conductivity, but are still only around $4^W/_{mK}$. The composites made with the same salts and alumina or magnesia have thermal conductivities not much lower than the graphite-based composites at around 2.5 or $3 ^W/_{mK}$. The thermal conductivity of the composites was not considered because at such low numbers, the conduction will not make a significant difference. A different system of analyzing the effective thermal conductivity would be needed to allow for the addition of heat conduction to the analysis.

The graphite-based composites with lithium carbonate and lithium nitrate have the highest heat capacities of the composites, but only by a slight margin. Each of the ceramics has a noticeable effect on the salt's heat capacity, but the effect is small in each case.

The thermal analysis shows almost identical temperature profiles for each composite of the same salt. As discussed previously, the heat capacities of the composites made with the same salt are minutely different, so the temperature output, which was based mostly on the heat capacity, would not be expected to be different.

The cost analysis showed a considerable difference between composites. The cost analysis did involve assuming that enough heat would be applied to the material to completely transform the salt to liquid and continue increasing the

composite's temperature. Therefore, the cost analysis is the best-case scenario for each composite. The analysis showed that the composite of alumina and sodium carbonate was the least expensive per kilowatt-hour, followed by the composite of magnesia and sodium carbonate at $79.03/kWh$_t$ and $91.34/kWh$_t$, respectively. While these prices are generally good for the system, the price requested in the EPSCoR survey response of $0.06/kWh$_e$ will not be reached using these materials.

In the future, an analysis that takes into account the differences in thermal conductivity between the composites would be extremely beneficial in this comparison. As seen in Chapter Four, the thermal conductivities varied enough to warrant further investigation.

Another possible future study would be constructing an actual block of salt-ceramic, which could be measured for the properties calculated in this paper. Being able to compare a realistic measurement to these calculations could shed light on whether these equations can practically be used to approximate the thermophysical properties.

Literature Cited

About zirconia [Internet]. K-Style Advanced Ceramics; c2006. Available from: http://zro2.com/

Barlev D, Vidu R, Stroeve P. 2011. Innovation in concentrated solar power. Solar Energy Materials & Solar Cells. 95:2703-2725.

Bauer T, Laing D, Tamme R. 2012. Characterization of sodium nitrate as phase change material. Int J Thermophys. 33:91-104.

Bauer T, Tamme R. Unpublished. PCM-graphite composites for high temperature thermal energy storage. Available from: http://talon.stockton.edu/eyos/energy_studies/content/docs/FINAL_PAPERS/8B-1.pdf.

Demirbas MF. 2006. Thermal energy storage and phase change materials. Energy Sources, Part B. 1:85-95.

Duffie JA, Beckman WA. 2006. Solar engineering of thermal processes, 3rd ed. Hoboken (NJ); John Wiley & Sons, Inc.

Fisher Scientific [Internet]. Thermo Fisher Scientific Inc.; c2012. Available from:

http://www.fishersci.com/ecomm/servlet/cmstatic?href=index.jsp&store=Scientific&segment=scientificStandard&storeId=10652

Forsberg CW, Peterson PF, Zhao H. 2007. High-temperature liquid-fluoride-salt

closed-Brayton-cycle solar power towers. Journal of Solar Energy Engineering.

129:141-146.

Gokon N, Inuta S, Yamashita S, Hatamachi T, Kodama T. 2009. Double-walled

reformer tubes using high-temperature thermal storage of molten-salt/MgO

composite for solar cavity-type reformer. International Journal of Hydrogen Energy.

34:7143-7154.

Graphite and composites [Internet]. UCSD. Available from:

http://aries.ucsd.edu/LIB/PROPS/PANOS/c.html

Graphite powder [Internet]. Reade. Available from:

http://www.reade.com/component/content/article/243-natural-graphite-powder-cas7782-42-5-synthetic-graphite-powder-cas7440-44-0-graphite-c-nano-graphite-plumbago-black-lead-nuclear-grade-graphite-mineral-carbon-silver-graphite-stove-black-stove-polish-electr?q=graphite+powder

Han JH, Cho KW, Lee KH, Kim H. 1998. Porous graphite matrix for chemical heat pumps. Carbon. 36(12):1801-1810.

Hoffman HW, Lones J. 1955. Fused salt heat transfer part II: forced convection heat transfer in circular tubes containing NaF-KF-LiF eutectic. Available from: http://www.osti.gov/energycitations/product.biblio.jsp?osti_id=4016896.

Holcomb DE, Cetiner SM. 2010. An overview of liquid-fluoride-salt heat transport systems. Available from: http://info.ornl.gov/sites/publications/Files/Pub25407.pdf

Huang J, Zhu D, Zhang R. 2009. Study on fabrication technology and melting heat transfer process of salt/ceramic composite phase change energy storage materials [paper]. In: International Conference on Energy and Environment Technology; 2009. p. 348-352.

Janz GJ. 1988. Thermodynamic and transport properties for molten salts: correlation equations for critically evaluated density, surface tension, electrical conductance, and viscosity data. Journal of Physical and Chemical Reference Data. 17(2).

Kaminski M. 2003. Homogenization of transient heat transfer problems for some composite materials. International Journal of Engineering Science. 41:1-29.

Kenisarin MM. 2010. High-temperature phase change materials for thermal energy

storage. Renewable and Sustainable Energy Reviews. 14:955-970.

Kourkova L, Sadovska G. 2007. Heat capacity, enthalpy and entropy of Li_2CO_3 at

303.15-653.15K. Thermochimica Acta. 452:80-81.

Li P, Van Lew J, Chan C, Karafi W, Stephens J, O'Brien JE. 2012. Similarity and

generalized analysis of efficiencies of thermal energy storage systems. Renewable

Energy. 39:388-402.

Lindberg D, Backman R, Chartrand P. 2007. Thermodynamic evaluation and

optimization of the (Na_2SO_4 + Na_2S + K_2CO_3 + K_2SO_4 +K_2S) system. J Chem

Thermodynamics. 39:942-960.

Lopez J, Acem Z, Palomo Del Barrio E. 2010. KNO_3/$NaNO_3$-Graphite materials for

thermal energy storage at high temperature: Part II-Phase transition properties.

Applied Thermal Engineering. 30:1586-1593.

Material: aluminum oxide [Internet]. MEMSnet. Available from:

https://www.memsnet.org/material/aluminumoxideal2o3bulk/

Pal R. On the Lewis-Nielsen model for thermal/electrical conductivity of composites. Composites: Part A. 39:718-726.

Pincemin S, Olives R, Py X, Christ M. 2008. Highly conductive composites made of phase change materials and graphite for thermal storage. Solar Energy Materials & Solar Cells. 92:603-613.

Progelhof RC, Throne JL, Ruetsch RR. 1976. Methods for predicting the thermal conductivity of composite systems: a review. Polymer Engineering and Science. 16(9):615-625.

Ren N, Wu Y, Wang T, Ma C. 2011. Experimental study on optimized composition of mixed carbonate for phase change thermal storage in solar thermal power plant. J Therm Anal Calorim. 104:1201-1208.

Sabharwall P, Ebner M, Sohal M, Sharpe P, Anderson M, Sridharan K, Ambrosek J, Olson L, Brooks P. 2010. Molten salts for high temperature reactors: University of Wisconsin molten salt corrosion and flow loop experiments- issues identified and path forward. Available from: http://www.coal2nuclear.com/Molten%20Salts%20For%20High%20Temperature%20Reactors%20-%204502649.pdf.

Skoropanov AS, Bulgak IA, Petrov GS, Gusev GS, Vecher AA. 1984. Heat capacities and thermal linear expansion coefficients of graphite intercalation compounds with $CuCl_2$ and $CoCl_2$. Synthetic Metals. 9:361-368.

Slifka AJ, Filla BJ, Phelps JM. 1998. Thermal conductivity of magnesium oxide from absolute, steady-state measurements. Journal of Research of the National Institute of Standards and Technology. 103(4):357-363.

Taha S, Abousehly AM, Attia G, El-Sharkawy AA. 1991. Measurement of thermophysical properties of KNO_3. Thermochimica Acta. 181:167-171.

Tojo T, Atake T. 1999. Heat capacity and thermodynamic functions of zirconia and yttria-stabilized zirconia. J Chem Thermodynamics. 31:831-845.

Wang J, Carson JK, North MF, Cleland DJ. 2006. A new approach to modeling the effective thermal conductivity of heterogeneous materials. International Journal of Heat and Mass Transfer. 49:3075-3085.

Wu Y, Ren N, Wang T, Ma C. 2011. Study on optimized composition of mixed carbonate salt for sensible heat storage in solar thermal power plant. Solar Energy. 85:1957-1966.

Yaws CL. 2009. Thermal conductivity of solid-inorganic compounds. Beaumont: William Andrew. Chapter 9, Transport properties of chemical and hydrocarbons; p. 403-406.

Yaws CL. 2009. Thermal conductivity of liquid-inorganic compounds. Beaumont: William Andrew. Chapter 8. Transport properties of chemical and hydrocarbons; p. 396-402.

Zabolotskii AV. 2011. Mathematical simulation of the thermal stability of magnesium oxide. Heat Engineering. 52(3):170-177.

Curriculum Vitae

Lauren Michelle Fossile

9304 Brilliant Ore Drive, Las Vegas, NV 89143

Employment History

University of Nevada, Las Vegas - Research Graduate Assistant

August 2010-August 2012

Las Vegas, Nevada

National Science Foundation-Experimental Program to Stimulate Competitive

Research grant: created and conducted a survey of the energy utilities in

Nevada concerning climate change

Chevron Corporation - Reliability Intern

Pascagoula, Mississippi

June 2008-September 2008

Education

University of Nevada, Las Vegas, Las Vegas, Nevada

Master of Science in Mechanical Engineering (2012)

California Polytechnic State University, San Luis Obispo, California

Bachelor of Science in Materials Engineering (2008)

Presentations

Poster Session. Energy Purveyors and Climate Change in Nevada: Knowledge, Needs, and Perspectives. Graduate Student Professional Association Research Forum. Las Vegas, Nevada. 2012.

Poster Session. Energy Purveyors and Climate Change in Nevada: Knowledge, Needs, and Perspectives. National Science Foundation-Experimental Program to Stimulate Competitve Research Tri-State Meeting. Sun Valley Idaho. 2012.

Poster Session. Energy Purveyors and Climate Change in Nevada: Knowledge, Needs, and Perspectives. National Science Foundation-Experimental Program to Stimulate Competitve Research Nevada State Meeting. Las Vegas, Nevada. 2012.

Paper Session. Energy Purveyors and Climate Change in Nevada: Knowledge, Needs, and Perspectives. Association of American Georgaphers Annual Meeting. New York, New York. 2012.

Poster Session. Perceptions, Preferences, and Attitudes of Nevada's Energy Utilities Regarding Climate Change. Association of American Geographers Annual Meeting. Seattle, Washington. 2011

Poster Session. Perceptions, Preferences, and Attitudes of Nevada's Energy Utilities Regarding Climate Change. National Science Foundation-Experimental Program to Stimulate Research Tri-State Meeting. Albuquerque, New Mexico. 2011.

Poster Session. Perceptions, Preferences, and Attitudes of Nevada's Energy Utilities Regarding Climate Change. Graduate Student Professional Assoication Research Forum. Las Vegas, Nevada. 2011.